JOURNAL OF
Materials
CHEMISTRY

The preparation and chemical structure of TiO_2 film photocatalysts supported on stainless steel substrates *via* the sol–gel method

Yongfa Zhu,* Li Zhang, Li Wang, Yan Fu and Lili Cao

Department of Chemistry, Tsinghua University, Beijing 100084, China.
E-mail: zhuyf@chem.tsinghua.edu.cn

Received 3rd January 2001, Accepted 11th April 2001
First published as an Advance Article on the web 15th May 2001

A compact TiO_2 film with a thickness of about 90 nm has been coated onto stainless steel substrates by using the sol–gel method with $Ti(OBu)_4$ as precursor. AES analysis showed that Fe diffused from the substrate into the TiO_2 film and reacted with O_2 from the air, resulting in the formation of an interlayer of iron oxide during the annealing process. XPS and XRD results indicate that the Fe in the TiO_2 layer and interlayer exists as a rhombohedral Fe_2O_3 species. With increasing annealing temperature and time, the diffusion can be significantly promoted. Although iron oxide did not react with TiO_2 film, the formation of anatase TiO_2 film was impeded due to the presence of Fe. It has been proven by UV spectroscopic analysis of TiO_2 film that Fe enters the TiO_2 lattice and changes the lattice parameters, resulting in a change in the optical properties of the TiO_2 film photocatalyst.

1 Introduction

Due to its photocatalytic activity under UV illumination, TiO_2 has been applied to a variety of problems of environmental interest. Its high efficiency, safety, cleanness and low cost have highlighted TiO_2 as a very promising catalyst.[1–5] However, because TiO_2 powder can not easily be separated from the suspension after degradation has occurred, TiO_2 film photocatalysts have become the focus of research concerning photocatalysts for the purification of liquid phases.[6–9] It was considered that film-type photocatalysts normally had lower photocatalytic activity than powders due to their lower surface area but by suitable preparation, TiO_2 film can show much higher photocatalytic activity than that of the most active commercial TiO_2 powders—Degussa P-25. Considering their stability and applicability, the film-type TiO_2 catalysts are of great technological importance. TiO_2 film photocatalysts can also be used to produce highly efficient solar-energy cells.[10,11] So far most of the research papers on TiO_2 film have only involved a study of the structure of the crystal phase, the catalytic reaction and so on. Discussions of the interface reaction between the photocatalyst film and the substrate, and the effect of the interface reaction on the structure and properties of the catalyst are needed since the interface reaction could have a serious influence on the properties of the photocatalyst.

In this study, TiO_2 film has been coated on 304 stainless steel plates by using the sol–gel method with $Ti(OBu)_4$ as precursor, and a study of the chemical structure and optical properties of the resulting TiO_2 film was carried out using AES, XRD and UV-VIS spectroscopy.

2 Experimental

2.1 Preparation of TiO_2 film

0.5 ml $Ti(OBu)_4$ (A.P.) was added, dropwise and at room temperature, into 15 ml EtOH (A.P.), then three drops of hydrolyst (HNO_3 : EtOH = 1 : 10) were added into the solution. After being stirred with an ultrasonic horn for 15 min, the resultant clear light yellow solution was sealed and gelatized for 5 days, yielding a viscous sol. The sol was coated onto a stainless steel substrate (cleaned with EtOH) using a spin-coating method (3000 rpm) to form a wet gel film. To prepare porous film, PEG400 (C.R.) was added into the precursor with a PEG : Ti ratio of 10%. After drying the sample at room temperature the film was annealed, in air, at different temperatures (350–550 °C) for 1 h to form TiO_2 film. To prevent cracking during film drying, the heating rate should be maintained at about 5 °C min^{-1}. Rhodamine B (about 10 μM) was used to evaluate the catalytic properties of the TiO_2 film. Oxygen was bubbled into the reactor with a flow rate of 40 ml min^{-1}. The film in the solution was illuminated with a black light (365 nm, 20 W).

2.2 Surface and interface characterization

The AES spectra were measured in a PHI 610 SAM system. A coaxial electron gun with a single pass cylindrical mirror analyzer (CMA) was used. The energy resolution of the CMA was set at 0.3% to obtain a good energy resolution. For AES analysis, the electron beam energy and the beam current were 3.0 keV and 0.5 μA, respectively. The beam size was less than 0.5 μm. The electron beam was incident at an angle of 60° with respect to the specimen surface. During the depth profile analysis, the energy and beam current of the Ar ion beam were 3.0 keV and 6 μA, respectively. The beam was focused on a spot with a diameter of about 1 mm, and the sputtering rate was about 30.0 nm min^{-1} for a thermally oxidized SiO_2 thin film.

The XPS spectra were measured in a PHI 5300 ESCA system. During XPS analysis, an Al-Kα X-ray beam was used, and the power was set at 250 W. A hemispherical analyzer with a position sensitive detector at a pass energy of 37.75 eV was used. The base vacuum of the chamber was maintained at 3×10^{-9} Torr during XPS analysis. XRD experiments were carried out in a Rigaku DMAX-2400 diffractometer using Cu-Kα radiation. UV spectra were recorded on a Shimadzu S2600 UV spectrometer.

DOI: 10.1039/b100048i

3 Results and discussion

3.1 Interaction between TiO_2 film and stainless steel substrate

To prepare a TiO_2 photocatalyst with an anatase structure from the precursor film, the sample must be calcined in air at high temperature (300–550 °C). Fig. 1A shows the AES depth profile spectrum of a TiO_2 film/stainless steel sample annealed at 400 °C for 1 h in air. As shown in Fig. 1A, the TiO_2 layer has a thickness of 90 nm and the distribution of Ti with depth is homogeneous. An interlayer between the TiO_2 film and the substrate can be observed and Fe can be found in the TiO_2 surface layer, the concentration of Fe in the TiO_2 layer is about 7 mol%. The above results suggest that there has been a significant diffusion between the TiO_2 film and the stainless steel substrate. Fe has diffused into the TiO_2 surface layer from the stainless steel to form an oxide during the annealing treatment. Two kinds of oxygen species can be extracted from the depth profile spectrum by using linear least squares (LLS) fitting of the O KLL spectra. In the surface layer, most of the oxygen exists as TiO_2 with a small amount as iron oxide. At the interface between TiO_2 and substrate oxygen, as Fe_2O_3, appears with a peak-like distribution, implying that iron oxide has formed during the annealing treatment. The formation of iron oxide is believed to result from the reaction between oxygen that has diffused into the interface with Fe that has diffused from the substrate. Cr and Ni can hardly be detected in the diffusion layer, which can be explained as it is much easier for Fe to react with oxygen. Thus the oxidation of Fe has promoted its diffusion into the TiO_2 film.

To clarify the distribution and chemical states of elements in the thin film, line shape analyses of the AES were carried out.[12] The Ti L_3MM spectra at various depths in the sample calcined at 400 °C for 1 h are shown in Fig. 1B. In the surface and interface layers, the line shapes of Ti L_3MM are the same. They consist of two peaks at 409.3 eV and 414.8 eV, which can be attributed to $L_3M_{23}M_4$ and $L_3M_1M_4$ of TiO_2. The line shapes are similar to those of the pure TiO_2 species, implying that the diffusion of iron oxide can not change the electronic structure of TiO_2, *i.e.* TiO_2 has not reacted with iron oxide. Since the line shape of Fe LMM is not sensitive to the chemical environment, it is impossible to identify the Fe species from the Fe LMM line shape. Cr can not be detected by Cr LMM until the interlayer (depth D) is reached. The Cr L_3MM spectra at various depths in the TiO_2/stainless steel sample are shown in Fig. 1C. In the surface layer (from depth A to C), there is a single peak at 488.4 eV, which can be attributed to O KLL of TiO_2. In the interface layer (from depth D to E), the peaks become very broad and can be fitted to two peaks. The kinetic energies are 485.7 eV and 488.4 eV, which can be attributed to pure Cr and oxygen in TiO_2. The above results indicate that Cr still exists as metallic Cr after annealing in air. Ni can not be detected until the interface between iron oxide interlayer and substrate (depth E) is reached. The kinetic energy of Ni LMM remains at 842.5 eV and the line shape is the same as that of Ni in the alloy, implying that Ni also exists in the metallic state.

Fig. 1D shows the Auger valence band spectra at various depths of the thin film. Several Auger peaks can be observed. The peaks with kinetic energies of 30.0 eV and 36.7 eV are attributed to the spectra of Cr MVV and Ti MVV, respectively. In fact, it can be seen that Ti exists as a TiO_2 species both on the surface and in the film. No reaction between TiO_2 and Fe has taken place because the line shape and the kinetic energy of Ti LMM are the same as those of standard TiO_2. Fe MVV peaks of Fe_2O_3 can also be observed at 37 eV and 43 eV, which are smaller than the kinetic energy of pure Fe (43.4 eV). Thus the Fe_2O_3 species are believed to exist as an interface layer in the thin film. In the interface layer, most of the Fe exists as Fe_2O_3 with some still in the metallic state. Cr can only be found as

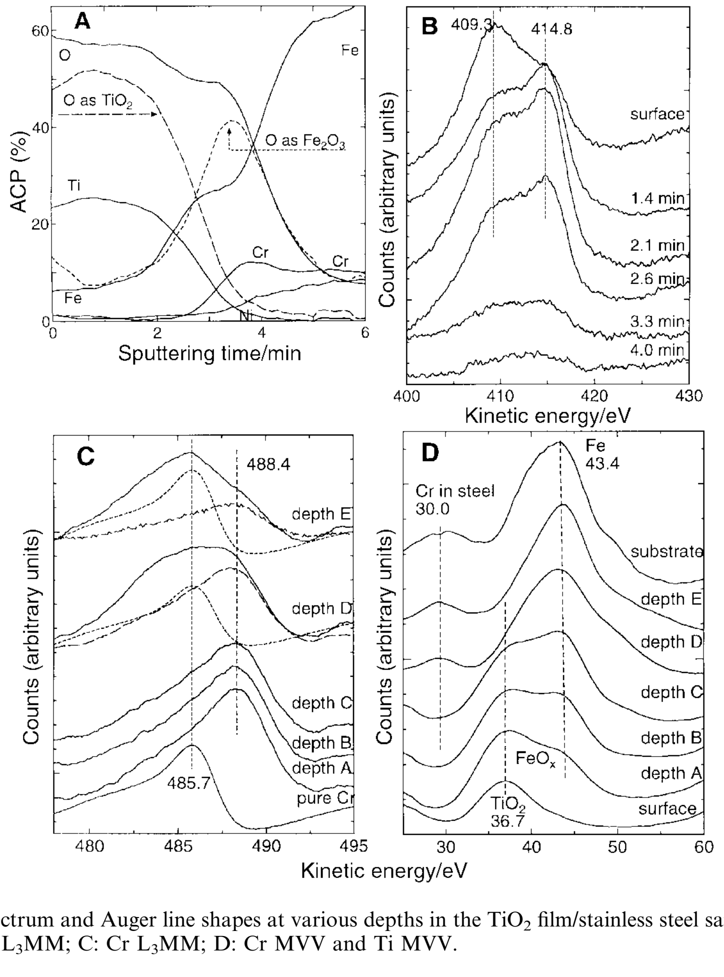

Fig. 1 The AES depth profile spectrum and Auger line shapes at various depths in the TiO_2 film/stainless steel sample annealed at 400 °C for 1 h. A: depth profile spectrum; B: Ti L_3MM; C: Cr L_3MM; D: Cr MVV and Ti MVV.

pure Cr at the interface of the Fe_2O_3 layer and substrate because Cr is not easily oxidized at low temperature. Based on the above result, no oxidation of Cr or Ni has taken place and only Fe has been oxidized during the formation of TiO_2.

The chemical states of elements on the surface layer have also been investigated by using XPS. Fig. 2 shows the Fe 2p spectra of the TiO_2 film/steel sample annealed at 500 °C for 1 h. On the surface of the sample, the binding energy of Fe $2p_{3/2}$ is 710.9 eV, which can be attributed to an Fe_2O_3 species. In addition, two shake-up peaks can be observed and the line shape is similar to that of the Fe_2O_3 species, implying that Fe exists as Fe_2O_3 on the surface of the TiO_2 film catalyst. After the film has been etched to *ca.* 15 nm by an Ar ion beam, the binding energy of Fe $2p_{3/2}$ decreases from 710.9 eV to 709.8 eV and the line shape is changed. The binding energy and line shape of Fe 2p corresponds to that of an FeO species. The FeO species results from the reduction of the Fe_2O_3 species due to ion bombardment.[13] Based on the results of XPS, it can be concluded that Fe exists in TiO_2 film as an Fe_2O_3 species.

3.2 The influence of annealing temperature and time on the interface diffusion and reaction

To study the influence of annealing temperature and time on the surface structure of the film and the interaction between the film and the steel substrate, the precursor film was annealed at different temperatures (350–550 °C) and for different lengths of time (1–8 h). Even at annealing temperatures as low as 350 °C, the AES depth profile spectrum indicated that the iron oxide interlayer could be formed at the interface between TiO_2 film and steel substrate. Iron oxide has also diffused into the TiO_2 surface layer and the concentration of Fe in the TiO_2 layer is about 5 mol%. With the annealing temperature rising, the diffusion is promoted. There is a considerable increase in the thickness of the interlayer and the concentration of Fe in the TiO_2 layer. When the sample is annealed at 550 °C for 1 h in air, the thickness of the oxide interlayer increases to about 79 nm and the concentration of Fe in the TiO_2 layer increases to about 10 mol%. Cr can be found in the diffusion layer, while Ni can not, which suggests that diffusion of Fe is still faster than that of other elements at high temperature. As shown in Fig. 1A, Fe has diffused not only into the TiO_2 film layer, but also into the surface of the film.

According to the above results, it can be concluded that annealing temperature has a serious effect on the chemical structure of the TiO_2 film. The Fe_2O_3 layer can be formed even at annealing temperatures as low as 350 °C. The formation of the diffusion layer and the diffusion of Fe into the TiO_2 film are certain to have a crucial influence on the properties of TiO_2 photocatalysts.

The thickness of the interface layer and the Fe concentration in the surface of samples calcined at various temperatures are shown in Table 1. As is shown, the depth of the interface layer increases with annealing temperature, which implies that the diffusion of Fe has been promoted. In fact, the diffusion of Fe results not only from the calcination but also from the chemical inducement of oxygen from the atmosphere. The latter is believed to be more crucial at low temperature. Most of the Cr and Ni remains in the substrate layer because they are not as easily oxidized as Fe.

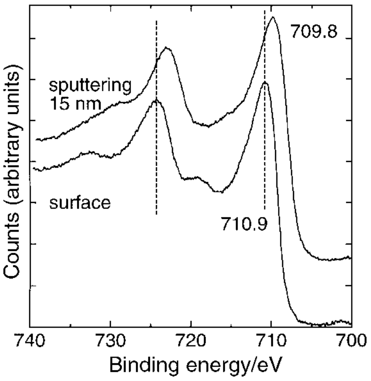

Fig. 2 The Fe 2 p spectra of a TiO_2 film/stainless steel sample annealed at 500 °C for 1 h.

Table 1 The influence of calcination temperature

Calcination temperature/°C	350	400	450	500	550
Interlayer thickness/nm	45.0	46.5	45.9	51.2	79.0
Concentration of Fe in the surface layer/mol%	5.0	7.1	7.8	8.2	10

Not only the annealing temperature but also the annealing time can have a serious influence on the chemical structure of the TiO_2 film. As seen in Table 2, the thickness of the diffusion layer does not increase markedly, which suggests that increasing annealing time has much less effect on the interface oxidation than increasing the annealing temperature. However, the amount of Fe in the TiO_2 film increases with annealing time, and the concentration of Fe can reach *ca.* 13 mol% in the TiO_2 film which implies that the diffusion of Fe into the TiO_2 film can be promoted by increasing the annealing time. Thus the annealing time also influences the properties of the TiO_2 film catalyst.

3.3 The crystalline structure of the TiO_2 film/steel sample

The crystalline structure of TiO_2 film/steel samples has been studied using XRD. Fig. 3 shows the XRD diffraction patterns of TiO_2 film/steel samples annealed at various temperatures. When the annealing temperature is low (350 °C), a strong peak can be observed at 44.54°, which results from the diffraction of stainless steel substrate. Several weak peaks can also be seen,

Table 2 The influence of calcination time

Calcination time/h	1	2	4	8
Interlayer thickness/nm	46.5	48.0	55.5	55.2
Concentration of Fe in the surface layer/mol%	7.1	8.2	10.6	12.6

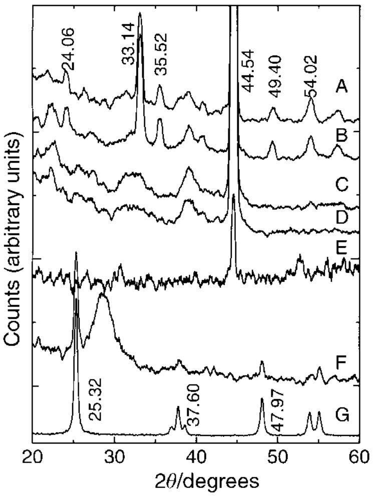

Fig. 3 The XRD patterns of TiO_2 film/stainless steel samples annealed at various temperatures for 1 h. A: stainless steel annealed at 500 °C; B: TiO_2/steel annealed at 500 °C; C: TiO_2/steel annealed at 400 °C; D: TiO_2/steel annealed at 300 °C; E: stainless steel; F: TiO_2/Si film annealed at 400 °C; G: anatase TiO_2.

but they do not correspond to the diffraction patterns of anatase TiO_2. These weak peaks can be attributed to an oxide of iron. With rising annealing temperature, several peaks appear at 24.06, 33.14, 35.52 and 54.02°, which can be attributed to a rhombohedral Fe_2O_3 phase. The peaks of Fe_2O_3 become intensified with annealing temperature, but the diffraction peaks of anatase TiO_2 can not be observed. Even if the annealing temperature is increased to 550 °C, the diffraction patterns of anatase TiO_2 can not be detected, implying that the formation of anatase TiO_2 film on stainless steel substrate can be impeded because of the diffusion of Fe into the TiO_2 film.

3.4 Influence of calcination on the optical properties of TiO_2 film

The photoreactivity of TiO_2 partly depends on the absorbency of UV light. To study the influence of calcination on the optical properties of TiO_2 film, the UV spectra of TiO_2 films annealed at different temperatures and for different lengths of time were obtained. As shown in Fig. 4, TiO_2 film on steel substrate has a relatively intensified absorbency for UV light compared to TiO_2 film on Si substrate. In the UV spectrum of steel annealed at 400 °C for 1 h, two peaks (enlarged by five times) can be observed at 325 nm and 430 nm, respectively. There is a considerable difference between the sample annealed at 350 °C and the steel substrate. Two peaks can be observed at 285 nm and 480 nm, respectively. Compared with the spectrum of TiO_2 film on Si substrate, these two peaks result from doped TiO_2 film. (There will be a red shift in the UV spectrum of doped TiO_2 film.) With rising temperature, there will not only be an intensification of the two peaks, but also a red shift from 285 nm and 480 nm at 350 °C to 318 nm and 680 nm at 550 °C. Compared with the spectrum of TiO_2 film and oxide layer on the surface of steel, the spectra of TiO_2 film on steel substrate result not from the total absorbency of the TiO_2 film and steel substrate, but also from the doped TiO_2 film. Considering the conclusion in section 3.1, the shift of wavelength probably results from the interaction between TiO_2 and Fe that has diffused into the TiO_2 film. Fe has entered the lattice of TiO_2 and changed the lattice parameters and crystal field structure. As to TiO_2, the absorption of UV light mainly results from the promotion of 3 d electrons in the crystal field. The change in lattice parameters for doped TiO_2 film is sure to affect the promotion of 3 d electrons, causing a change in the absorption spectrum. Since the diffusion of Fe can be increased with temperature, the change in the lattice parameters of TiO_2 becomes more pronounced as the annealing temperature is increased, resulting in an increasing shift in wavelength.

The influence of annealing time on the UV spectra was also studied. Fig. 5 shows the UV spectra of TiO_2 film annealed at 400 °C for different periods of time. With increasing annealing time, a red shift and intensification of two peaks can be observed. When the annealing time is increased from 1 h to 4 h, the wavelength of the two peaks shift from 290 nm and 530 nm to 310 nm and 580 nm, respectively. The change of UV spectra can also be explained with the discussion in section 3.1. As shown in Table 2, when increasing annealing time, the thickness of the Fe_2O_3 layer hasn't obviously increased, while the amount of Fe that has diffused into the TiO_2 film increases greatly, which shows that both the intensification and red shift of the UV peaks can not result from the change of the oxide layer, but from diffusion of Fe into the TiO_2 film. To make a further comparison, the sample coated twice has also been annealed at 400 °C for 1 h. As shown in Fig. 5, a weak absorbency and a red shift can be observed. It shows that with increasing thickness of the compact film, the UV absorbency of the doped diffusion layer is weakened, while the red shift still takes place because the interaction between Fe and TiO_2 film is not affected by the thickness of the TiO_2 film.

It can also be seen in Figs. 4 and 5 that the TiO_2 film on steel substrate has a remarkable absorption in the visible region. However, absorption in this area is useless in terms of photocatalysis because TiO_2 can only be active under the illumination of UV light that has a spectrum less than 380 nm. To evaluate the photocatalytic activity of TiO_2 films on steel substrates, Rhodamine B solution has been degraded using a TiO_2 film catalyst. No change in Rhodamine concentration was observed on irradiation with visible light, which suggests that TiO_2 can not be activated by low energy radiation. Even if illuminated with UV light (365 nm, 20 W), there were only slight decreases in Rhodamine concentration after 3 h due to the low surface area of the compact TiO_2 film. To increase the surface area, porous film has been prepared by the addition of PEG to the precursor. Fig. 6 shows that the degradation can be greatly promoted when the surface area is increased.

4 Conclusion

A compact TiO_2 film has been coated onto a stainless steel substrate by using the sol–gel method with $Ti(OBu)_4$ as precursor. A significant interface diffusion of Fe, together with the formation of an Fe_2O_3 interlayer, can be detected after the annealing treatment, resulting in a doped TiO_2 film. The diffusion of Fe into the TiO_2 film can be promoted by

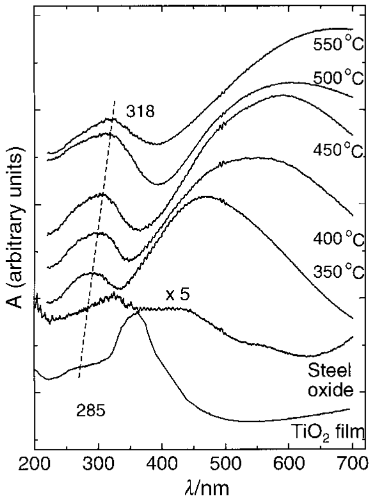

Fig. 4 The UV spectra of TiO_2 film/stainless steel samples annealed at various temperatures for 1 h.

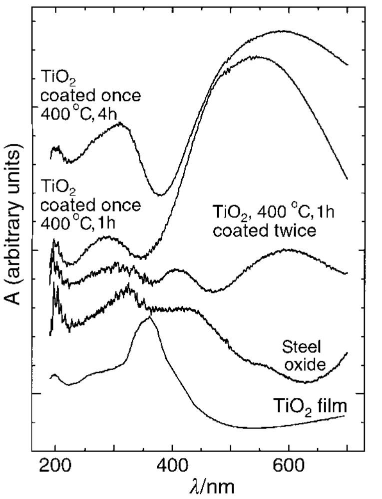

Fig. 5 The UV spectra of a TiO_2 film/stainless steel sample annealed at 400 °C for 1 h and 4 h.

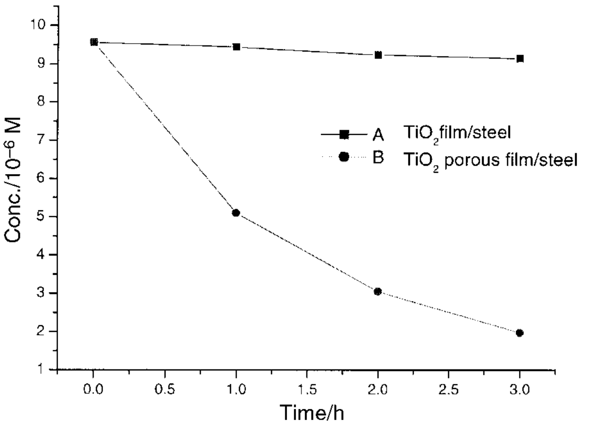

Fig. 6 The degradation of Rhodamine B using TiO_2 film under UV radiation. A: TiO_2 film on stainless steel substrate; B: TiO_2 porous film on stainless steel substrate.

increasing the annealing temperature and time. The diffusion of Fe into the TiO_2 film impedes the formation of anatase TiO_2 film. Compared to TiO_2 film on Si substrates, the UV absorption of TiO_2 film on steel substrate can be intensified and a red shift can be observed, which results from the change of lattice parameters caused by the diffusion of Fe into the TiO_2 lattice. The intensification and red shift of peaks can be strengthened when the annealing temperature and time are increased due to the promotion of the diffusion of Fe.

Acknowledgements

This work was partly supported by a Grant-in Aid for Scientific Fundamental Research of Tsinghua University Visiting Scholar Foundation of Key Lab in University, and sponsored by Scientific Research Foundation for Returned Overseas Chinese Scholars, Minister of Education.

References

1 N. Negishi, T. Iyoda, K. Hashimoto and A. Fujishima, *Chem. Lett.*, 1995, 841.
2 M. R. Hoffmann, S. T. Martin, W. Choi and D. W. Bahnemann, *Chem. Rev.*, 1995, **95**, 69.
3 X. Fu, W. Zeltner and M. A. Anderson, *Appl. Catal. B*, 1995, 209.
4 D. F. Oills, E. Pelizzetti and N. Serpone, *Environ. Sci. Technol.*, 1991, **25**, 1522.
5 Y. Zhu, L. Zhang, C. Gao and L. Cao, *J. Mater. Sci.*, 2000, **35**, 4049.
6 K. Tennakone and I. R. M. Kottegoda, *J. Photochem. Photobiol. A: Chem.*, 1996, **93**, 79.
7 Y. Zhu, L. Zhang, W. Yao and L. Cao, *Appl. Surf. Sci.*, 2000, **158**, 32.
8 Y. Zhu, L. Zhang, L. Wang, Y. Fu and L. Cao, *Acta Chim. Sin.*, 2000, **58**, 467.
9 I. Sopyan, M. Watanabe, S. Murasawa, K. Hishimoto and A. Fujishima, *J. Photochem. Photobiol. A: Chem.*, 1996, 69.
10 U. Bach, D. Lupo, P. Comte, J. E. Moser and F. Weissertel, *Nature*, 1998, **395**, 583.
11 B. O'regan and M. Gratzel, *Nature*, 1991, **353**, 737.
12 Y. Zhu and L. Cao, *Appl. Surf. Sci.*, 1998, **133**, 213.
13 N. S. McIntyre and D. G. Zetaruk, *Anal. Chem.*, 1977, **49**, 1521.